Biomaterials 33 (2012) 3539–3547

Contents lists available at SciVerse ScienceDirect

Biomaterials

journal homepage: www.elsevier.com/locate/biomaterials

Biologic scaffolds composed of central nervous system extracellular matrix

Peter M. Crapo [1], Christopher J. Medberry [1], Janet E. Reing, Stephen Tottey, Yolandi van der Merwe, Kristen E. Jones, Stephen F. Badylak*

McGowan Institute for Regenerative Medicine, University of Pittsburgh, Pittsburgh, PA 15219, USA

ARTICLE INFO

Article history:
Received 11 January 2012
Accepted 25 January 2012
Available online 14 February 2012

Keywords:
Extracellular matrix
Central nervous system
Scaffolds
Decellularization
Regenerative medicine
Tissue engineering

ABSTRACT

Acellular biologic scaffolds are commonly used to facilitate the constructive remodeling of three of the four traditional tissue types: connective, epithelial, and muscle tissues. However, the application of extracellular matrix (ECM) scaffolds to neural tissue has been limited, particularly in the central nervous system (CNS) where intrinsic regenerative potential is low. The ability of decellularized liver, lung, muscle, and other tissues to support tissue-specific cell phenotype and function suggests that CNS-derived biologic scaffolds may help to overcome barriers to mammalian CNS repair. A method was developed to create CNS ECM scaffolds from porcine optic nerve, spinal cord, and brain, with decellularization verified against established criteria. CNS ECM scaffolds retained neurosupportive proteins and growth factors and, when tested with the PC12 cell line in vitro, were cytocompatible and stimulated proliferation, migration, and differentiation. Urinary bladder ECM (a non-CNS ECM scaffold) was also cytocompatible and stimulated PC12 proliferation but inhibited migration rather than acting as a chemoattractant over the same concentration range while inducing greater rates of PC12 differentiation compared to CNS ECM. These results suggest that CNS ECM may provide tissue-specific advantages in CNS regenerative medicine applications and that ECM scaffolds in general may aid functional recovery after CNS injury.

1. Introduction

The extracellular matrix (ECM) represents the secreted product of the resident cells of each tissue and organ and thus logically defines the ideal substrate or scaffold for maintenance of tissue-specific cell phenotype. The ECM is a critical determinant of cell behavior and is known to affect intracellular signaling pathways, cell differentiation events, and cell proliferation among other important characteristics of tissue identity [1–8]. These events are mediated through integrins and other cell surface receptors in response to ligands present within the ECM of every tissue [9–11]. Subtle changes in ECM structure and mechanical properties can affect cell transcriptional events and associated cell phenotype and function [12,13].

Biologic scaffolds composed of ECM have been commonly used for the therapeutic reconstruction of many tissues including myocardium [14–16], kidney [17], lower urinary tract [18,19], musculotendinous tissues [20–22], esophagus [23], and peripheral nerve [24], among others. There is clinical precedent for the application of ECM scaffolds in reconstruction of central nervous system (CNS) structures [25,26], but the development of ECM scaffolds for CNS regenerative medicine strategies has received relatively scarce attention [27–29]. It has been suggested that ECM harvested from specific tissues is the preferred substrate for cells native to those respective tissues if maintenance of phenotypic characteristics is important [3–8,30]. The methods by which ECM scaffolds are prepared vary greatly and such methods can markedly affect the composition, architecture, and material properties of the resulting construct [31–34] as well as the host response following implantation [35–38]. Therefore, the methods of preparing ECM scaffolds intended for use in the repair and reconstruction of complex vital tissues such as heart, liver, kidney, and the CNS must be carefully considered as regenerative medicine strategies are developed for these tissues and organs.

The objectives of the present study were to (1) develop a method for decellularization of a variety of CNS tissues, (2) characterize the resulting CNS ECM scaffolds in terms of composition and in vitro cytocompatibility, and (3) investigate potential

* Corresponding author. Tel.: +1 412 235 5144; fax: +1 412 235 5110.
E-mail address: badylaks@upmc.edu (S.F. Badylak).
[1] These authors contributed equally to this work.

0142-9612/$ – see front matter © 2012 Elsevier Ltd. All rights reserved.
doi:10.1016/j.biomaterials.2012.01.044

tissue-specific advantages of CNS ECM scaffolds compared to non-CNS ECM scaffolds by evaluating in vitro modulation of PC12 cell line mitogenesis, chemotaxis, and differentiation.

2. Materials and methods

2.1. Preparation of CNS ECM

Porcine optic nerve, spinal cord, and brain tissues were obtained from animals (~120 kg) at a local abattoir (Thoma's Meat Market, Saxonburg, PA). Tissues were frozen (>16 h at −80 °C), thawed completely, and separated from all non-CNS tissue. Dura mater was removed, and optic nerve and spinal cord tissues were longitudinally quartered and cut into lengths (<3 cm). The decellularization process consisted of a series of agitated baths: water (type I reagent water per ASTM D1193; 16 h at 4 °C; 60 rpm), 0.02% trypsin/0.05% EDTA (60 min at 37 °C) (Invitrogen Corp., Carlsbad, CA, USA), 3.0% Triton X-100 (60 min) (Sigma-Aldrich Corp., St. Louis, MO, USA), 1.0 M sucrose (15 min) (Fisher Scientific, Pittsburgh, PA, USA), water (15 min), 4.0% deoxycholate (60 min) (Sigma), 0.1% peracetic acid (Rochester Midland Corp., Rochester, NY, USA) in 4.0% ethanol (120 min), PBS (15 min) (Fisher), water (15 min), water (15 min), and PBS (15 min). Agitation speed was 200 rpm for optic nerve and spinal cord tissues or 120 rpm for brain tissue with the exception of the initial step at 60 rpm. Decellularized optic nerve (Fig. 1A), spinal cord (Fig. 1B), and brain (Fig. 1C) were lyophilized and stored dry until use.

2.2. Characterization of CNS ECM constituents

2.2.1. Characterization of residual DNA in CNS ECM

Qualitative assessment of residual DNA [31,39] was conducted by fixation of non-lyophilized ECM scaffolds in 10% neutral buffered formalin, which was then embedded in paraffin, sectioned, and stained with hematoxylin and eosin (H&E) or with 4′,6-diamidino-2-phenylindole (DAPI). Quantitative analysis of DNA content and base pair length in the remaining CNS ECM was conducted by digestion of comminuted ECM with 0.1 mg/ml proteinase K solution (48–144 h). Protein was removed by repeated phenol/chloroform extraction and centrifugation (10,000g) until no white precipitate (protein) was observed at the interface, and the aqueous phase extract was mixed with 3 M sodium acetate and 100% ethanol. The solution was centrifuged to pellet DNA, and the pellet was rinsed with 70% ethanol, centrifuged, and dried. Double-stranded DNA was quantified using PicoGreen (Invitrogen) per kit instructions. Base pair length of residual DNA in CNS ECM scaffolds was determined by gel electrophoresis of DNA extracts on 1.0% agarose gel with ethidium bromide (2 h at 60 V) followed by imaging with ultraviolet transillumination. Decellularization was evaluated against established criteria: (1) absence of visible nuclei in H&E and DAPI stained sections; (2) no DNA fragments exceeding 200 bp in length; and (3) <50 ng dsDNA per mg lyophilized ECM [31].

2.2.2. Protein content of CNS ECM

Unstained sections of native (non-decellularized) optic nerve, spinal cord, and brain and their respective ECM were deparaffinized, rehydrated, and stained for myelin via luxol fast blue [40] or immunostained for laminin via citrate antigen retrieval, blocking with 2% normal goat serum, incubation with rabbit anti-human laminin primary antibody (diluted 1:25; Sigma, L9393), H_2O_2, goat anti-rabbit IgG peroxidase-conjugated secondary antibody (diluted 1:400; Sigma, A0545), and diaminobenzidine (ImmPACT DAB substrate; Vector Laboratories Inc., Burlingame, CA, USA), followed by hematoxylin counterstaining and ethylene-xylene dehydration.

Growth factors were extracted from 30 to 50 mg comminuted ECM per ml buffer by one of two methods. The first method used 50 mM Tris containing 2.0 M urea, 5.0 mg/ml heparin, and protease inhibitors [41], and the second method used 20 mM Tris containing 1.0% NP40, 10% glycerol, and protease inhibitors. Vascular endothelial growth factor (VEGF) and basic fibroblast growth factor (bFGF) were assayed in urea-heparin extracts, while nerve growth factor (NGF) was assayed in NP40-glycerol extracts. Growth factors were quantified via Quantikine Human VEGF Immunoassay (R&D Systems Inc., Minneapolis, MN, USA), Quantikine Human FGF basic Immunoassay (R&D Systems), and NGF Emax ImmunoAssay System (Promega Corp., Madison, WI, USA) per manufacturer instructions. Primary and secondary extracts were obtained and assayed separately, with results summated. Growth factor analysis was indicative of concentration but not activity. Urinary bladder ECM was prepared as described previously [42] and used as a reference material.

2.3. In vitro characterization of CNS ECM

The pheochromocytoma-derived PC12 cell line (CRL-1721; ATCC, Manassas, VA, USA), a neoplastic rat cell line arising from neural crest tissue [43], was used as a model neural-like cell to evaluate in vitro modulation of mitogenesis, chemotaxis, and differentiation by ECM derived from decellularized CNS tissues. Urinary bladder ECM was again used as a reference material (i.e. non-CNS tissue source) to determine whether CNS ECM scaffolds offered any tissue-specific advantages. For in vitro cell assays, individual ECM samples were comminuted into particles (<1.0 mm) and solubilized with 1.0 mg/ml pepsin in 0.01 N HCl (Fisher). Protein concentrations were assayed in multiple dilutes of solubilized ECM against a bovine serum albumin standard curve using bicinchoninic acid. Each pepsin-HCl ECM solution was neutralized to pH 7.4 with 0.1 N NaOH (Fisher), isotonically balanced with 10X PBS (Fisher), and diluted to desired concentrations with 1X PBS. Mitogenic and chemotactic effects of ECM on PC12 cells were assayed for a range of concentrations (2.5, 10, 25, or 100 μg protein per ml), and PBS and/or neutralized pepsin lacking ECM served as controls in all assays. All in vitro assays were conducted as three or more replicates in triplicate or quadruplicate per condition.

Undifferentiated PC12 cells (P5-9) were passaged at 30–90% confluence on flasks coated with poly-L-lysine (PLL) in complete culture medium containing RPMI 1640 supplemented with 10% heat-inactivated horse serum (Sigma), 5.0% fetal bovine serum (FBS; Thermo Fisher Scientific Inc., Waltham MA, USA), and 100 U/ml penicillin/100 μg/ml streptomycin (pen/strep). To determine potential cytotoxic effects of ECM scaffolds, PC12 cells were plated on PLL-coated sterile glass coverslips at 70,000 cells per well in 12-well plates. ECM or PBS was added to the medium at 100 μg/ml 2 h after plating and cells were cultured for an additional 24 h. Cytocompatibility was determined using a Live/Dead Viability Kit (Invitrogen) per manufacturer instructions using 4.0 μM calcein AM and 4.0 μM ethidium homodimer-1. Viability of PC12 cells was quantified in fluorescence images using ImageJ (NIH) to split red and green channels, threshold, and count particles (cells), with binning to differentiate between cell clusters of various counts. The same ImageJ macro was used to analyze all images.

Mitogenic effects of CNS ECM scaffolds were determined by plating undifferentiated PC12 cells on PLL-coated 96-well plates at 4000 cells per well. After 12 h, ECM or PBS was added to each well and cells were cultured for another 20 h, followed by culture for 4.0 h with 5-bromo-2′-deoxyuridine (BrdU) and quantification of BrdU incorporation into PC12 DNA using a colorimetric BrdU cell proliferation ELISA (Roche Diagnostics Corp., Indianapolis, IN, USA) per manufacturer instructions.

Chemotactic effects of CNS ECM scaffolds were determined by transmembrane migration using blind-well chambers and polycarbonate filters with 8.0 μm pore size (AP48; Neuro Probe Inc., Gaithersburg, MD, USA). Filters were coated in 30 μg/ml laminin (Sigma) for 30 min and allowed to dry completely. Undifferentiated PC12 cells were cultured to 70–90% confluence, starved overnight in RPMI 1640 supplemented with 1.0% FBS (Thermo Fisher) and pen/strep, trypsinized, and resuspended in unsupplemented 50:50 RPMI 1640:PBS. Each ECM was brought to concentration with PBS and diluted 50:50 with RPMI 1640, with 10% FBS in RPMI 1640 used to verify chemotaxis through each filter. Wells were loaded with 40,000 cells per well, and after 6 h each filter was removed, the upper (non-migratory) surface scraped, and the lower

Fig. 1. Biologic scaffolds derived from porcine CNS tissues. (A) Native optic nerve tissue (left) and optic nerve ECM (right). (B) Native spinal cord tissue (left) and spinal cord ECM (right). (C) Native brain tissue (left) and brain ECM (right). All tissues and ECM are shown in their lyophilized state. Ruler divisions are 1.0 mm.

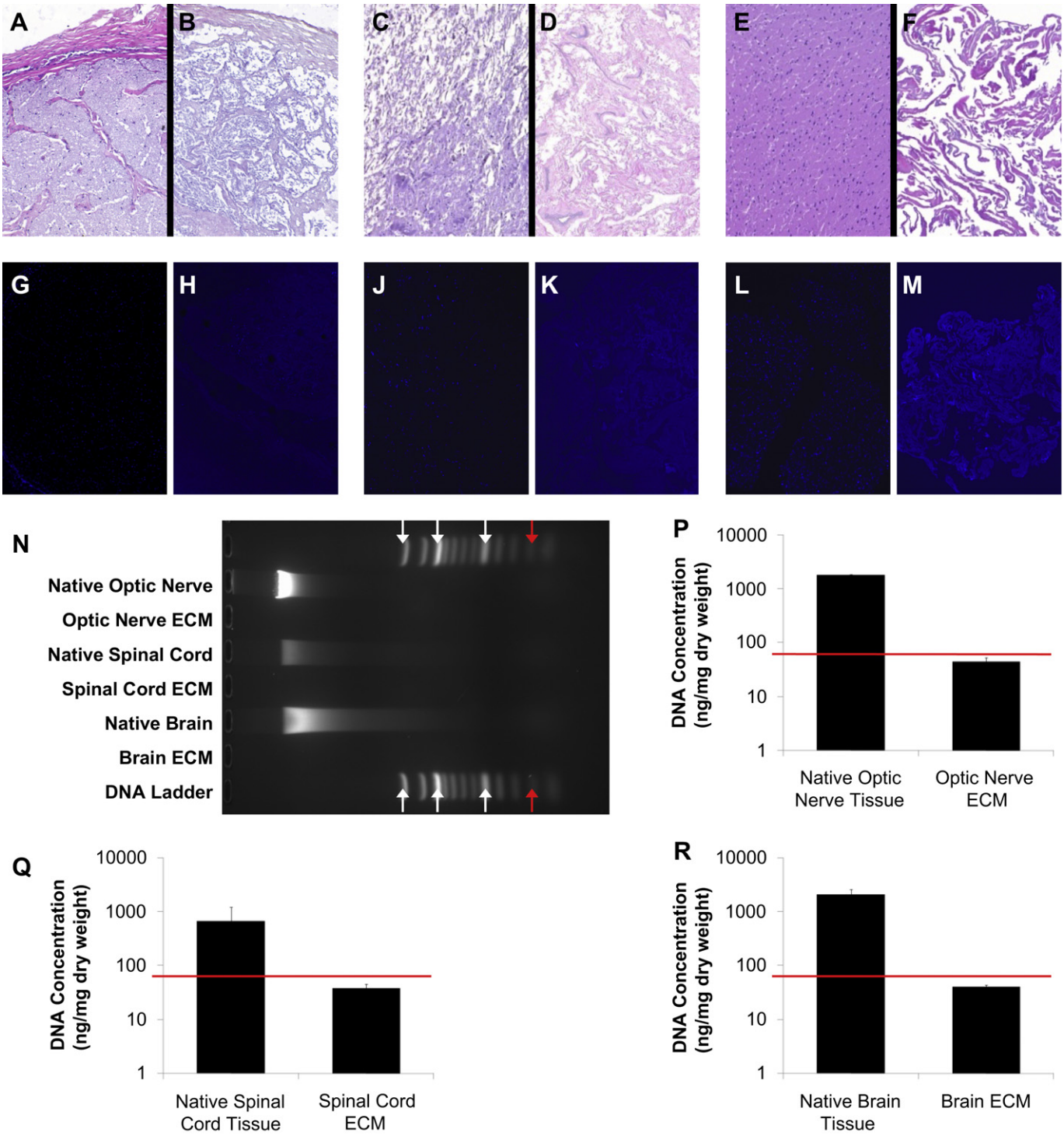

Fig. 2. Characterization of residual DNA in CNS ECM scaffolds. After H&E staining, cell nuclei were visible in (A) native optic nerve tissue but not in (B) optic nerve ECM. Cell nuclei were also visible in (C) native spinal cord tissue but not in (D) spinal cord ECM and in (E) native brain tissue but not in (F) brain ECM. DAPI showed similar results in (G) native optic nerve compared to (H) optic nerve ECM, (J) native spinal cord compared to (K) spinal cord ECM, and (L) native brain compared to (M) brain ECM. Magnification is 100×. (N) Gel electrophoresis showed that residual DNA fragments did not exceed 200 bp in optic nerve ECM, spinal cord ECM, or brain ECM. Arrows denote (left-right) 1500 bp, 1000 bp, 500 bp, and 200 bp (red arrows). (P–R) DNA quantification showed lower concentrations of DNA in CNS ECM compared to native tissues, with <50 ng DNA per mg ECM dry weight for decellularized optic nerve, spinal cord, and brain (note y axis is log scale; $n = 3$ for all groups; $p < 0.005$ for each native-ECM pair). Red lines denote established DNA criteria against which decellularization was verified [31]. (For interpretation of the references to colour in this figure legend, the reader is referred to the web version of this article.)

(migratory) surface fixed with methanol, stained with DAPI, and imaged. Cells were quantified using ImageJ to threshold and count cells, with binning to differentiate between cell clusters of various counts. The same ImageJ macro was used to analyze all images.

Differentiation effects of CNS ECM scaffolds were determined by plating PC12 cells at low density (1500 cells per well) in PLL-coated 48-well plates. After 6 h for attachment, cells were starved for 16 h in 1.0% heat-inactivated horse serum with pen/strep. bFGF [44], ECM, or PBS was added 50:50 to medium in each well to obtain desired final concentrations, and cells were cultured for another 48 h followed by fixation with paraformaldehyde, permeabilization with 0.1% Triton X-100, actin staining with Fluorescein-conjugated phalloidin, and imaging with a Zeiss AxioObserver Z1 microscope. The percentage of differentiated cells was determined by manually quantifying cells with at least one neurite-like process longer than the soma diameter, with a minimum of 300 cells counted per well [45,46].

2.4. Statistical analysis

Graphical representations of all data show mean ± standard deviation of at least three replicates, each conducted in triplicate or quadruplicate. Experimental groups depicted graphically as a pair were compared using a Student's *t*-test. All other groupings were compared using one-way analysis of variance (ANOVA) with Tukey–Kramer post hoc analysis. Outliers greater than three standard deviations from the mean were excluded from data sets.

3. Results

3.1. Efficacy of decellularization method

No residual nuclei were visible in H&E and DAPI images of ECM derived from optic nerve, spinal cord, or brain (Fig. 2A–M). Maximum fragment size of residual DNA in CNS ECM scaffolds did not exceed 200 bp (Fig. 2N) [31]. Quantification of dsDNA using PicoGreen showed that CNS ECM scaffolds retained <50 ng dsDNA per mg dry ECM (Fig. 2P–R). Concentrations of dsDNA were 44.6 ± 7.9 ng/mg in optic nerve ECM, 37.9 ± 7.7 ng/mg in spinal cord ECM, and 40.2 ± 3.8 ng/mg in brain ECM.

3.2. CNS ECM constituents

Histologic staining and immunohistochemistry showed that CNS ECM scaffolds each retained laminin and myelin present in native tissues (Fig. 3A–C). Optic nerve ECM, spinal cord ECM, and brain ECM also retained detectable concentrations of VEGF and bFGF, which were present in their tissues of origin (Fig. 4A,B). Concentrations of VEGF and bFGF in CNS ECM scaffolds were comparable to concentrations in a non-CNS ECM scaffold derived from urinary bladder. In contrast, although all native CNS tissues contained NGF, only optic nerve ECM retained a detectable concentration of NGF (Fig. 4C).

3.3. In vitro characterization of CNS ECM

Optic nerve ECM, spinal cord ECM and brain ECM were cytocompatible in vitro, as was a non-CNS ECM derived from urinary bladder (Fig. 5). Both CNS and non-CNS ECM scaffolds increased undifferentiated PC12 cell mitogenesis up to 1.5-fold in vitro at the concentrations tested (Fig. 6). CNS ECM scaffolds induced PC12 chemotaxis in vitro, resulting in up to 1.5-fold migration compared to unstimulated cells (Fig. 7A–C). In contrast, a non-CNS ECM scaffold attenuated migration to 0.5-fold control (Fig. 7D). Under the conditions assayed, CNS ECM scaffolds induced PC12 differentiation at rates approaching 20% while a non-CNS ECM scaffold induced differentiation at rates approaching 30% at an equivalent protein concentration (Fig. 8). In summary, all PC12 cell functions except viability were modulated by CNS and non-CNS ECM scaffolds, including mitogenesis, chemotaxis, and differentiation.

4. Discussion

This study describes a versatile decellularization method which can be applied to three different CNS tissues: optic nerve,

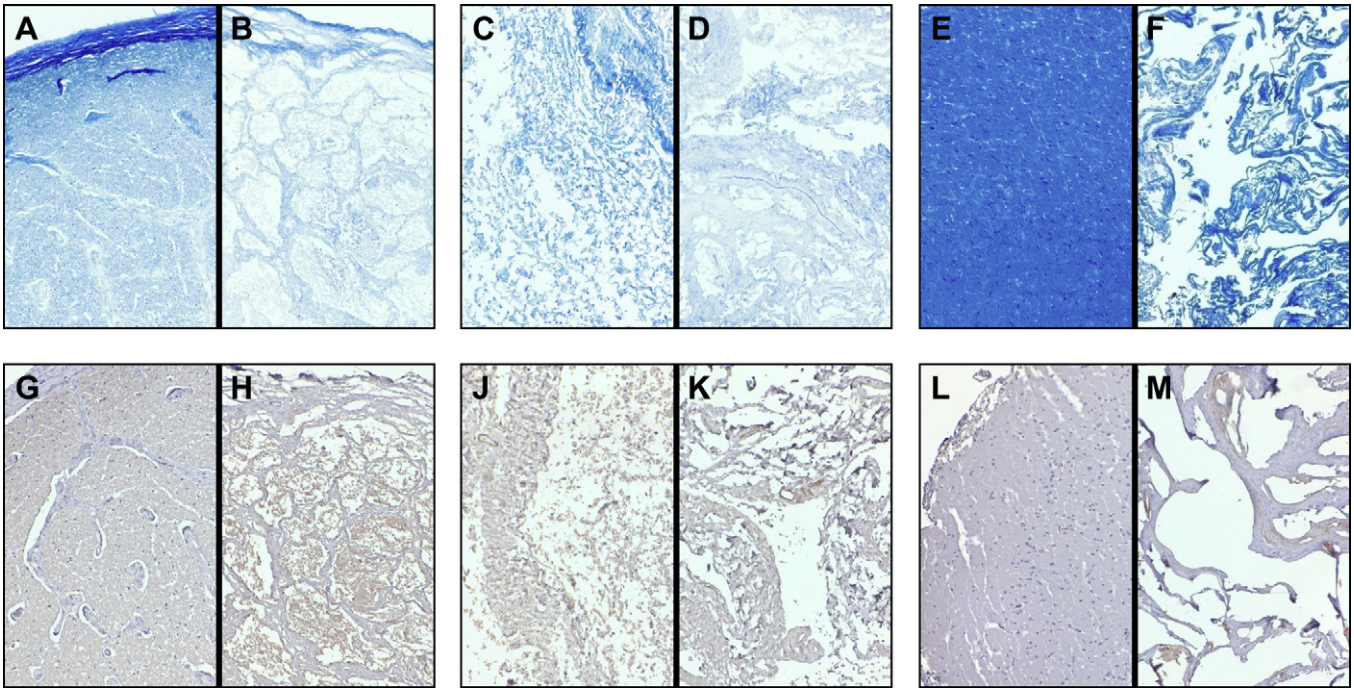

Fig. 3. Protein content of CNS ECM scaffolds. Myelin was present in (A) native optic nerve tissue, (B) optic nerve ECM, (C) native spinal cord tissue, (D) spinal cord ECM, (E) native brain tissue, and (F) brain ECM as shown by luxol fast blue staining. Laminin was also present in (G) native optic nerve, (H) optic nerve ECM, (J) native spinal cord, (K) spinal cord ECM, (L) native brain, and (M) brain ECM as shown by immunohistochemistry with hematoxylin counterstain. Magnification is 100×. (For interpretation of the references to colour in this figure legend, the reader is referred to the web version of this article.)

spinal cord, and brain (Fig. 1). The full protocol from tissue to ECM requires <24 h, a duration which compares favorably to previously reported CNS tissue decellularization methods [27–29]. The resulting matrix is sufficiently acellular (Fig. 2) to obviate adverse host immune responses [35–38] and contagion such as virus transmission [47–49] while retaining bioactive molecules, including myelin and laminin (Fig. 3). In vitro modulation of PC12 cell functions by CNS ECM (Figs. 6–8) and the matrices' retention of neurosupportive proteins as well as growth factors, including neuroinductive bFGF and the neurotrophin NGF (Fig. 4B,C), suggest that the materials might influence behavior of other neural and neural-like cells in vitro and in vivo.

Although the activity of growth factors, including neurotrophins, in CNS ECM scaffolds is unknown, similar PC12 responses to all three types of CNS ECM in vitro (Figs. 5–8) and the singular presence of NGF in optic nerve ECM (Fig. 4) suggests three non-exclusive possibilities: the amounts of NGF and other neurotrophins and growth factors (such as bFGF) with preserved bioactivity in each ECM are equivalent; spinal cord ECM and brain ECM contain higher concentrations of neurotrophins other than NGF which counterbalance greater NGF content in optic nerve ECM; or, most likely, each CNS ECM contains a unique profile of potent neurotrophins and growth factors which, in combination, yield similar effects. Indeed, subtle but forceful differences in constituent profiles might explain variability in PC12 mitogenesis and chemotaxis at the highest tested concentration of optic nerve ECM when compared to spinal cord or brain ECM (Figs. 6,7). Attenuation or even reversal of cell responses to optic nerve ECM at increasing concentrations (Figs. 6A and 7A) correlate well with other studies that have shown inhibitory cellular responses to segments of optic nerve compared to peripheral nerve in vitro [50] and in vivo [51].

Previous reports of ECM scaffolds derived from CNS tissues [27–29] have not explored tissue-specific functionality of these materials in contrast to non-CNS ECM. The present study clearly shows distinct cellular responses to CNS versus non-CNS ECM scaffolds, including divergent chemotactic and differentiation effects (Figs. 7,8) but similar mitogenic effects (Fig. 6). These results mimic the ability of other non-CNS ECM scaffolds to support site-appropriate cell phenotype in several complex tissues [4–8] and suggest unique capabilities for CNS ECM that may prove useful in regenerative medicine applications within the CNS.

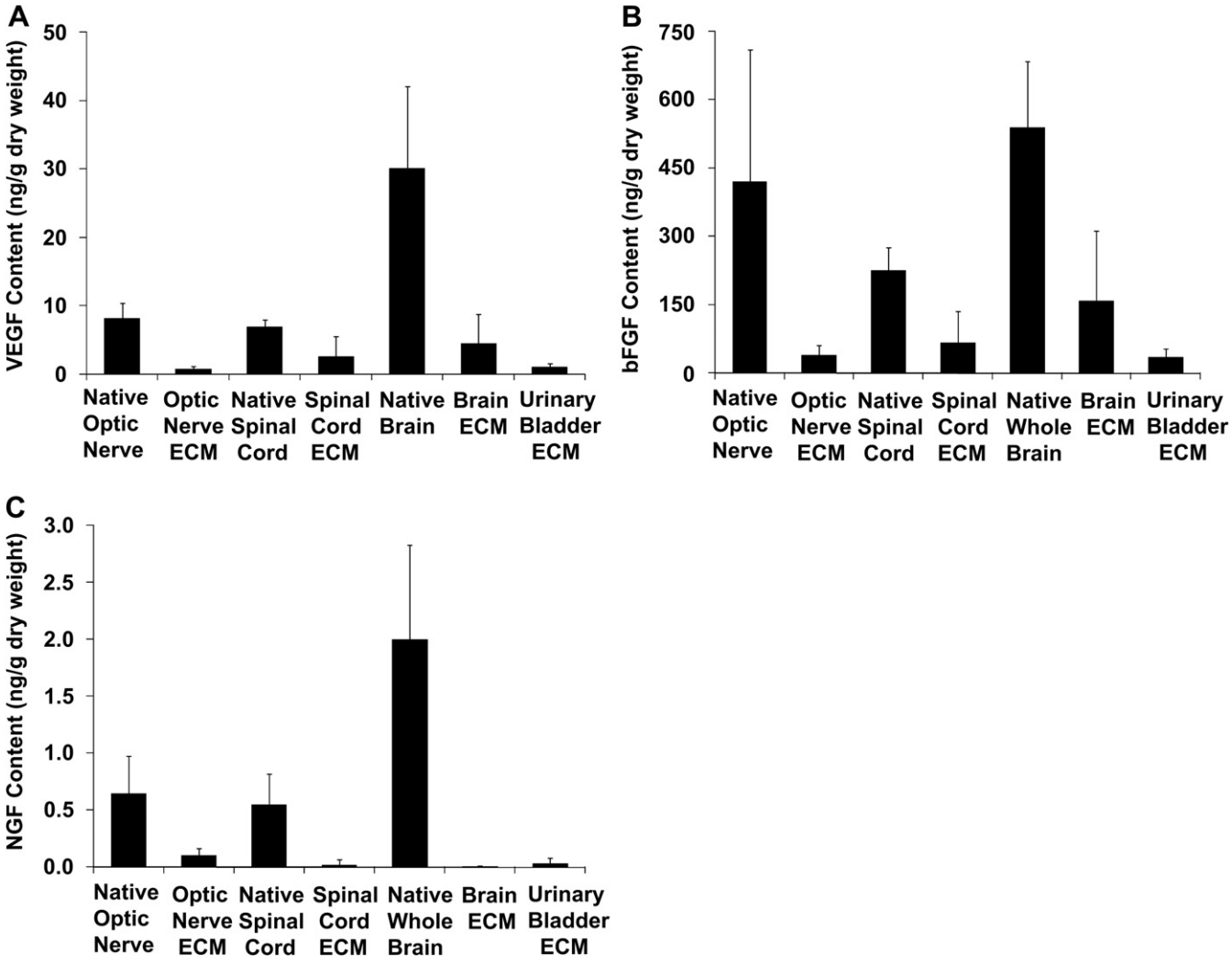

Fig. 4. Growth factor content of CNS ECM scaffolds. Optic nerve ECM, spinal cord ECM, brain ECM, and urinary bladder ECM retained detectable concentrations of (A) VEGF and (B) bFGF, which were also present in native tissues ($n = 3–5$). (C) Optic nerve ECM was the only matrix that retained a detectable concentration of NGF ($n = 3–4$).

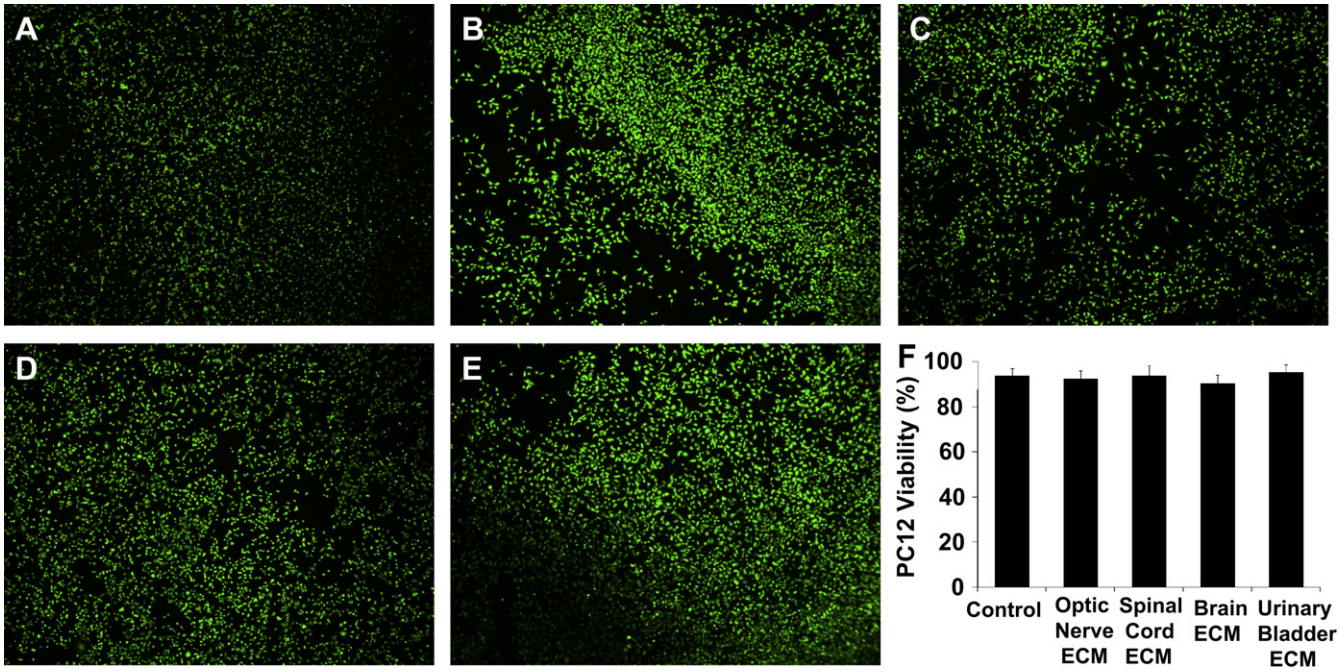

Fig. 5. Cytocompatibility of CNS ECM scaffolds. (A) Normal viability of undifferentiated PC12 cells was not different from viability of PC12 cells cultured with (B) optic nerve ECM, (C) spinal cord ECM, (D) brain ECM, or (E) urinary bladder ECM as determined by Live/Dead assay, including (F) quantification of live and dead cells in images. Cells were cultured in each ECM at a concentration of 100 μg protein per ml medium. Magnification is 400×.

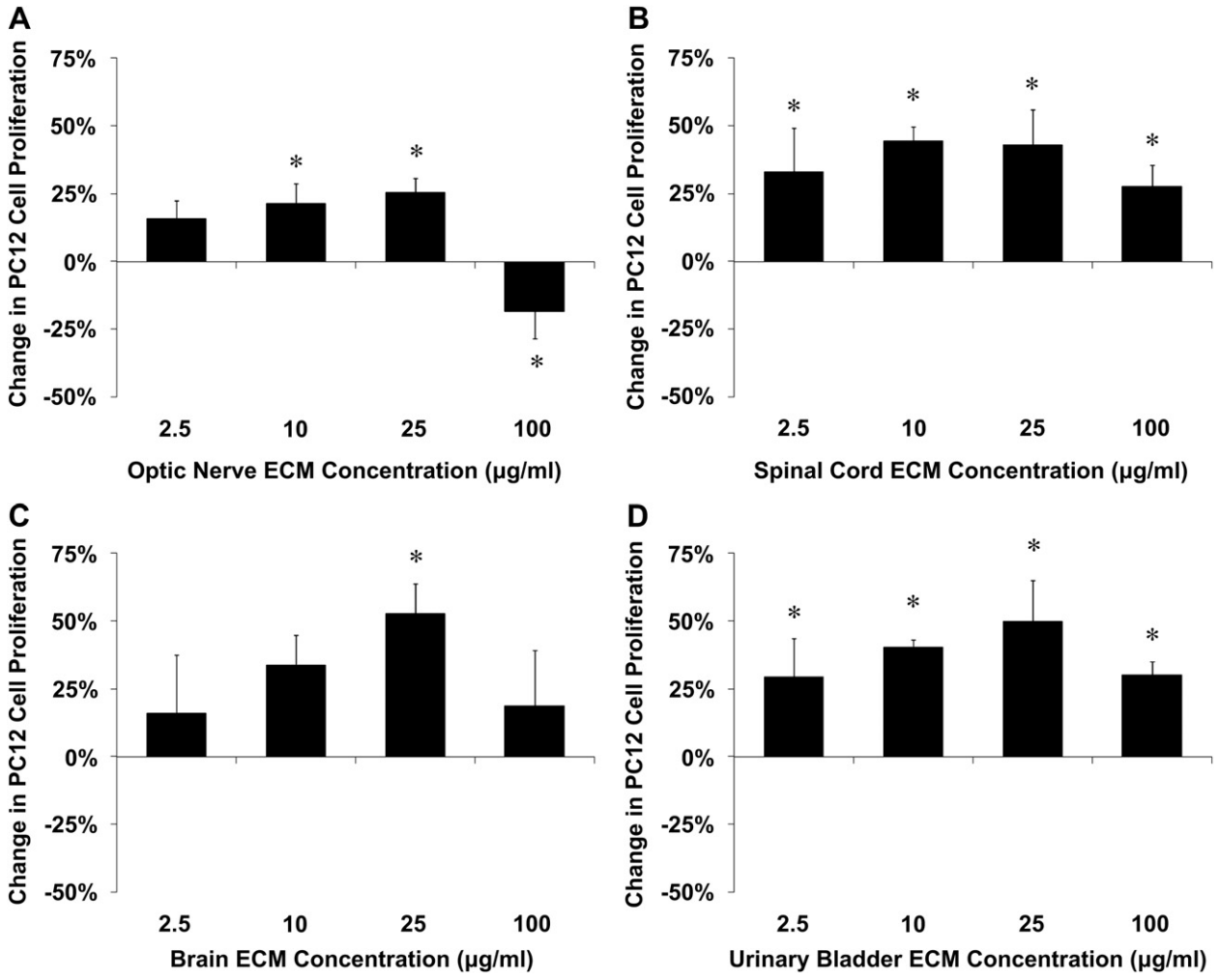

Fig. 6. Mitogenic effects of CNS ECM scaffolds. Undifferentiated PC12 cell proliferation was modulated by (A) optic nerve ECM, (B) spinal cord ECM, (C) brain ECM, and (D) urinary bladder ECM as determined by BrdU incorporation during PC12 cell mitosis. Changes in mitogenesis ranged from increases of 53% (brain ECM, 25 μg protein per ml) to decreases of 18% (optic nerve ECM, 100 μg protein per ml). * Indicates $p < 0.05$ by one-way ANOVA with Tukey–Kramer post hoc analysis.

Mitogenic and chemotactic effects of ECM scaffolds observed in this study were non-linear and generally conformed to an inverted-U curve commonly observed in neural cell responses to stimuli (Figs. 6,7) [52–54]. Increasing differentiation rates correlated with moderating mitogenic and chemotactic effects at higher ECM concentrations (Figs. 6–8), suggesting a dose-dependent shift in cellular responses. The establishment of ECM cytocompatibilities at 100 μg/ml (Fig. 5), the highest concentration used for any in vitro assay, further reinforced the concept that higher ECM concentrations caused alterations in cell behavior rather than apoptosis or functional impairment. Increased differentiation which coordinated with increased mitogenesis and chemotaxis at the same ECM concentration may indicate sub-populations of PC12 cells which respond differently to the ECM scaffolds or may reflect the complexity of each ECM composition as it influenced behavior of pluripotent cells [43]. In considering this phenomenon, it is important to note that the differentiation assay used unique conditions, including starvation medium, greater duration, and lower cell density. Overall, responses of PC12 cells to ECM scaffolds in vitro suggest that these materials might be used in vivo to control neural cell plasticity without adversely affecting viability.

Cell responses observed in this and other studies [2,3,42,55,56] suggest that ECM placed in vivo has the potential [43] to attract endogenous progenitors such as neural stem cells to a site of CNS damage, induce proliferation, and cause differentiation into functional, site-appropriate cells to replace lost CNS tissue in cases of injury or neurodegenerative pathologies. If CNS ECM proves to have advantages for in vivo constructive remodeling of CNS tissues, then gel forms of the scaffolds which cross-link in situ would logically be desirable for minimally invasive application in the CNS. Ultimately and perhaps ideally, delivery of ECM (CNS or non-CNS) to a site of CNS injury in cases such as stroke or spinal cord injury might be achieved by localized injection of an ECM gel [57] which would jointly fill the lesion, recruit endogenous stem cells, including neural stem cells, and enhance their regenerative responses [56]. Gel forms of ECM have been shown to induce rapid cell infiltration and site-appropriate constructive remodeling in vivo [16,58]. ECM scaffold remodeling in vivo is likely to be further aided by the presence of VEGF and bFGF within the scaffolds (Fig. 4A,B), which suggests potential to promote neovascularization. Development of a microvascular network would not only support new tissue formation via transport but could also deliver ECM degradation products as a signal to surrounding cells

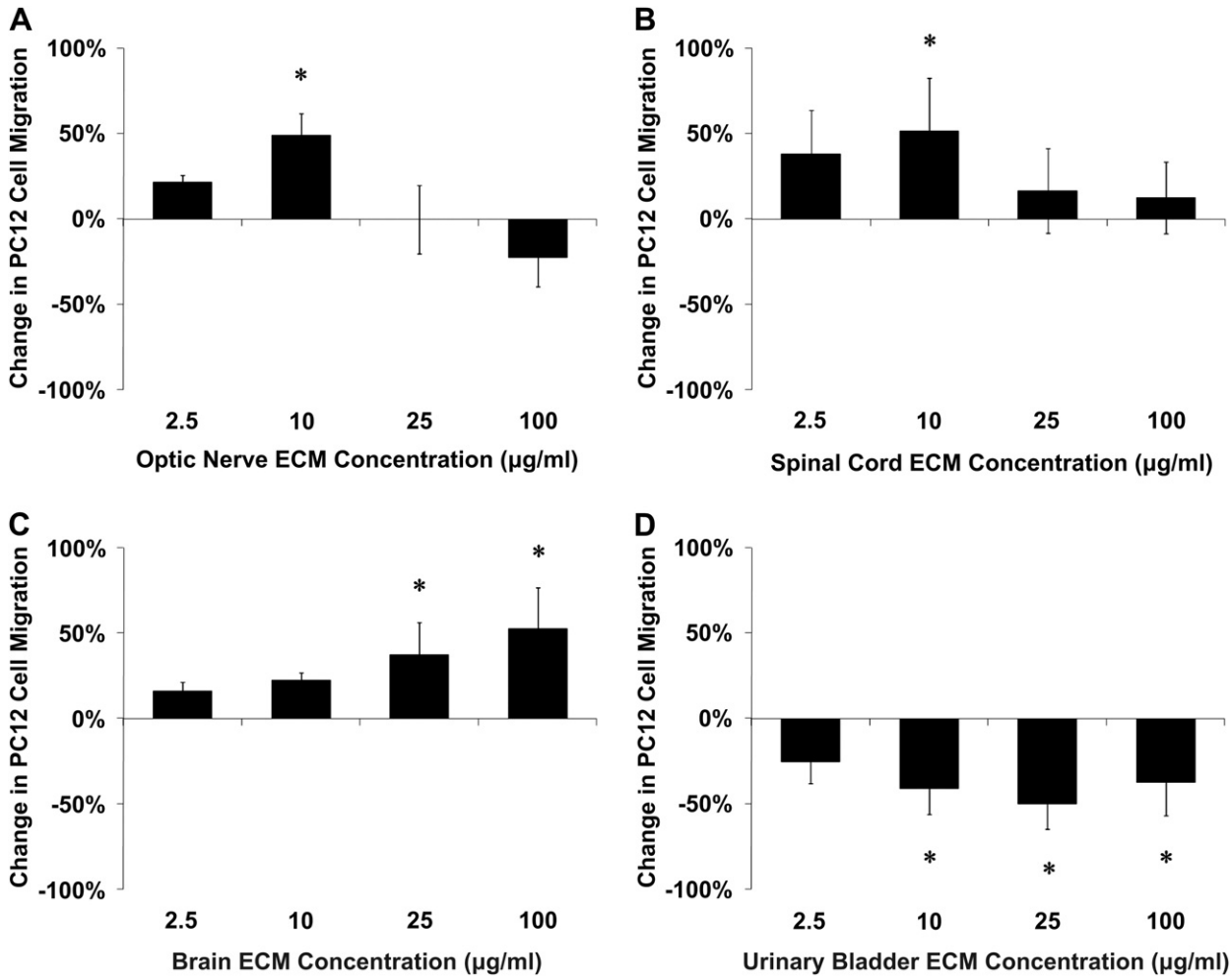

Fig. 7. Chemotactic effects of CNS ECM scaffolds. Undifferentiated PC12 cell migration was modulated by (A) optic nerve ECM, (B) spinal cord ECM, (C) brain ECM, and (D) urinary bladder ECM as determined by trans-membrane PC12 cell migration. Changes in chemotaxis ranged from increases of 53% (brain ECM, 100 μg protein per ml) to decreases of 50% (urinary bladder ECM, 25 μg protein per ml). * Indicates $p < 0.05$ by one-way ANOVA with Tukey–Kramer post hoc analysis.

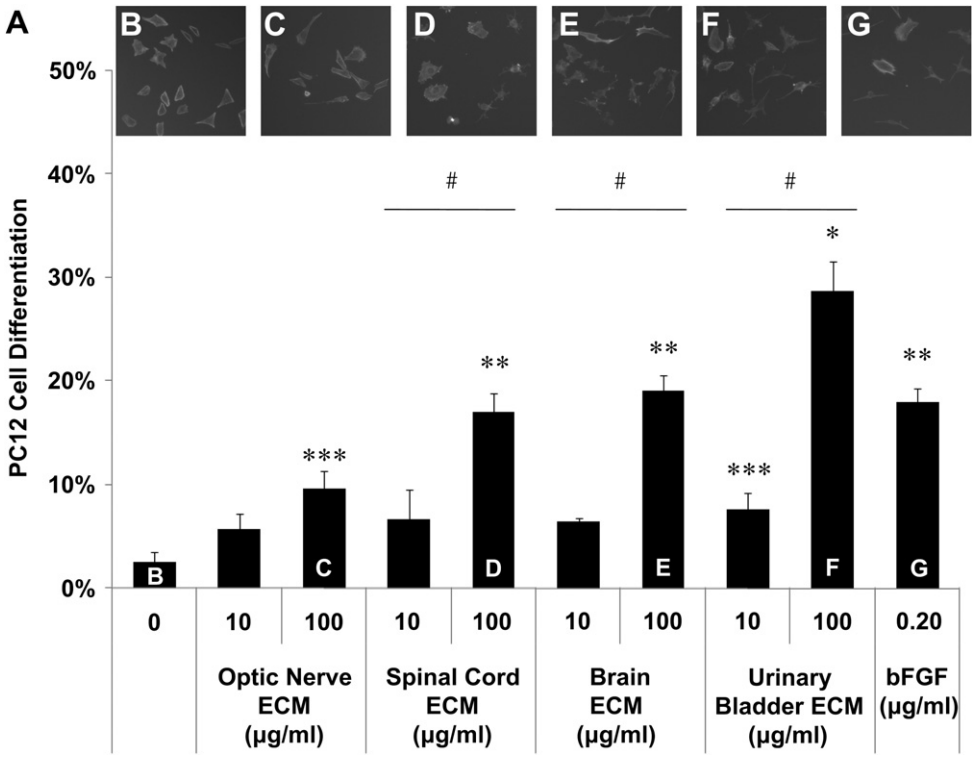

Fig. 8. Differentiation effects of CNS ECM scaffolds. (A) PC12 neuronal differentiation induced by CNS and non-CNS ECM as indicated by neurite extension. Differentiation was compared using the following medium supplements: (B) PBS as a negative control, (C) optic nerve ECM at 100 μg/ml, (D) spinal cord ECM at 100 μg/ml, (E) brain ECM at 100 μg/ml, urinary bladder ECM at 100 μg/ml, or (G) bFGF at 0.20 μg/ml as a positive control. * Urinary bladder ECM at 100 μg protein per ml induced greater differentiation than any other condition including the positive control (bFGF, 0.20 μg/ml). ** Spinal cord ECM or brain ECM at 100 μg/ml induced differentiation at rates comparable to the positive control which were greater than all other conditions except urinary bladder ECM at 100 μg protein per ml. *** Optic nerve ECM at 100 μg protein per ml or urinary bladder ECM at 10 μg protein per ml induced differentiation at greater rates than the negative control (no ECM: 0 μg/ml). # Differentiation rates increased with concentration for spinal cord ECM, brain ECM, and urinary bladder ECM (10 μg protein per ml vs. 100 μg protein per ml). Significant differences were determined between all groups shown by one-way ANOVA with Tukey–Kramer post hoc analysis ($p < 0.05$).

[42,56], thereby inducing constructive remodeling and functional CNS recovery.

5. Conclusion

A variety of acellular biologic scaffolds can be derived from CNS tissues such as optic nerve, spinal cord, and brain by a combination of enzymatic and chemical processing (Figs. 1,2). These CNS ECM scaffolds meet or exceed established decellularization criteria [31], are cytocompatible (Fig. 5), and retain neurosupportive proteins and growth factors present within the tissues of origin (Figs. 3,4) which are known to modify neural cell behaviors. The resultant acellular biologic scaffolds are able to modulate behaviors of model neural-like cell as demonstrated by increased proliferation, migration, and differentiation of the PC12 cell line in vitro over a range of concentrations (Figs. 6–8). Contrasting PC12 cell migration and differentiation responses to CNS versus non-CNS ECM suggest tissue-specific functionality for biologic scaffolds in neural applications. Overall, results of the study suggest that CNS and non-CNS ECM scaffolds may represent effective substrates for constructive neural tissue remodeling in vivo and facilitate regenerative medicine approaches to CNS repair.

Acknowledgments

This work was supported in part by the NIH (NIH) (5R01AR053603), an Ocular Tissue Engineering and Regenerative Ophthalmology (Ocular Tissue Engineering and Regenerative Ophthalmology) (OTERO) Fellowship from the Louis J. Fox Center for Vision Restoration (a joint program of UPMC and the University of Pittsburgh), and an NIBIB training (NIBIB training) grant (T32EB001026). The authors also thank Deanna Rhoads for histologic sectioning and Chris Carruthers for experimental assistance.

References

[1] Calve S, Odelberg SJ, Simon HG. A transitional extracellular matrix instructs cell behavior during muscle regeneration. Dev Biol 2010;344:259–71.
[2] Vorotnikova E, McIntosh D, Dewilde A, Zhang J, Reing JE, Zhang L, et al. Extracellular matrix-derived products modulate endothelial and progenitor cell migration and proliferation in vitro and stimulate regenerative healing in vivo. Matrix Biol 2010;29:690–700.
[3] Cortiella J, Niles J, Cantu A, Brettler A, Pham A, Vargas G, et al. Influence of acellular natural lung matrix on murine embryonic stem cell differentiation and tissue formation. Tissue Eng Part A 2010;16:2565–80.
[4] Ott HC, Clippinger B, Conrad C, Schuetz C, Pomerantseva I, Ikonomou L, et al. Regeneration and orthotopic transplantation of a bioartificial lung. Nat Med 2010;16:927–33.
[5] Zhang Y, He Y, Bharadwaj S, Hammam N, Carnagey K, Myers R, et al. Tissue-specific extracellular matrix coatings for the promotion of cell proliferation and maintenance of cell phenotype. Biomaterials 2009;30:4021–8.
[6] Sellaro TL, Ravindra AK, Stolz DB, Badylak SF. Maintenance of hepatic sinusoidal endothelial cell phenotype in vitro using organ-specific extracellular matrix scaffolds. Tissue Eng 2007;13:2301–10.
[7] Lin P, Chan WC, Badylak SF, Bhatia SN. Assessing porcine liver-derived biomatrix for hepatic tissue engineering. Tissue Eng 2004;10:1046–53.
[8] Wicha MS, Lowrie G, Kohn E, Bagavandoss P, Mahn T. Extracellular matrix promotes mammary epithelial growth and differentiation in vitro. Proc Natl Acad Sci U S A 1982;79:3213–7.
[9] Nelson CM, Bissell MJ. Of extracellular matrix, scaffolds, and signaling: tissue architecture regulates development, homeostasis, and cancer. Annu Rev Cell Dev Biol 2006;22:287–309.
[10] Gassmann P, Enns A, Haier J. Role of tumor cell adhesion and migration in organ-specific metastasis formation. Onkologie 2004;27:577–82.

[11] Bissell MJ, Radisky DC, Rizki A, Weaver VM, Petersen OW. The organizing principle: microenvironmental influences in the normal and malignant breast. Differentiation 2002;70:537–46.
[12] Barkan D, Green JE, Chambers AF. Extracellular matrix: a gatekeeper in the transition from dormancy to metastatic growth. Eur J Cancer 2010;46:1181–8.
[13] Bonneh-Barkay D, Wiley CA. Brain extracellular matrix in neurodegeneration. Brain Pathol 2009;19:573–85.
[14] Wainwright JM, Hashizume R, Fujimoto KL, Remlinger NT, Pesyna C, Wagner WR, et al. Right ventricular outflow tract repair with a cardiac biologic scaffold. Cells Tissues Organs 2012;195:159–70.
[15] Quarti A, Nardone S, Colaneri M, Santoro G, Pozzi M. Preliminary experience in the use of an extracellular matrix to repair congenital heart disases. Interact Cardiovasc Thorac Surg 2011;13:569–72.
[16] Singelyn JM, DeQuach JA, Seif-Naraghi SB, Littlefield RB, Schup-Magoffin PJ, Christman KL. Naturally derived myocardial matrix as an injectable scaffold for cardiac tissue engineering. Biomaterials 2009;30:5409–16.
[17] O'Connor RC, Harding 3rd JN, Steinberg GD. Novel modification of partial nephrectomy technique using porcine small intestine submucosa. Urology 2002;60:906–9.
[18] Palminteri E, Berdondini E, Colombo F, Austoni E. Small intestinal submucosa (SIS) graft urethroplasty: short-term results. Eur Urol 2007;51:1695–701. discussion 1701.
[19] Badylak SF, Kropp B, McPherson T, Liang H, Snyder PW. Small intestinal submucosa: a rapidly resorbed bioscaffold for augmentation cystoplasty in a dog model. Tissue Eng 1998;4:379–87.
[20] Butler CE, Langstein HN, Kronowitz SJ. Pelvic, abdominal, and chest wall reconstruction with AlloDerm in patients at increased risk for mesh-related complications. Plast Reconstr Surg 2005;116:1263–75. discussion 1276–1277.
[21] Mase Jr VJ, Hsu JR, Wolf SE, Wenke JC, Baer DG, Owens J, et al. Clinical application of an acellular biologic scaffold for surgical repair of a large, traumatic quadriceps femoris muscle defect. Orthopedics 2010;33:511.
[22] Turner NJ, Yates Jr AJ, Weber DJ, Qureshi IR, Stolz DB, Gilbert TW, et al. Xenogeneic extracellular matrix as an inductive scaffold for regeneration of a functioning musculotendinous junction. Tissue Eng Part A 2010;16:3309–17.
[23] Badylak SF, Hoppo T, Nieponice A, Gilbert TW, Davison JM, Jobe BA. Esophageal preservation in five male patients after endoscopic inner-layer circumferential resection in the setting of superficial cancer: a regenerative medicine approach with a biologic scaffold. Tissue Eng Part A 2011;17:1643–50.
[24] Karabekmez FE, Duymaz A, Moran SL. Early clinical outcomes with the use of decellularized nerve allograft for repair of sensory defects within the hand. Hand (N Y) 2009;4:245–9.
[25] Bejjani GK, Zabramski J. Safety and efficacy of the porcine small intestinal submucosa dural substitute: results of a prospective multicenter study and literature review. J Neurosurg 2007;106:1028–33.
[26] Haq I, Cruz-Almeida Y, Siqueira EB, Norenberg M, Green BA, Levi AD. Postoperative fibrosis after surgical treatment of the porcine spinal cord: a comparison of dural substitutes. Invited submission from the Joint Section Meeting on Disorders of the Spine and Peripheral Nerves, March 2004. J Neurosurg Spine 2005;2:50–4.
[27] Ribatti D, Conconi MT, Nico B, Baiguera S, Corsi P, Parnigotto PP, et al. Angiogenic response induced by acellular brain scaffolds grafted onto the chick embryo chorioallantoic membrane. Brain Res 2003;989:9–15.
[28] Guo SZ, Ren XJ, Wu B, Jiang T. Preparation of the acellular scaffold of the spinal cord and the study of biocompatibility. Spinal Cord 2010;48:576–81.
[29] DeQuach JA, Yuan SH, Goldstein LS, Christman KL. Decellularized porcine brain matrix for cell culture and tissue engineering scaffolds. Tissue Eng Part A 2011;17:2583–92.
[30] Stern MM, Myers RL, Hammam N, Stern KA, Eberli D, Kritchevsky SB, et al. The influence of extracellular matrix derived from skeletal muscle tissue on the proliferation and differentiation of myogenic progenitor cells ex vivo. Biomaterials 2009;30:2393–9.
[31] Crapo PM, Gilbert TW, Badylak SF. An overview of tissue and whole organ decellularization processes. Biomaterials 2011;32:3233–43.
[32] Freytes DO, Stoner RM, Badylak SF. Uniaxial and biaxial properties of terminally sterilized porcine urinary bladder matrix scaffolds. J Biomed Mater Res B Appl Biomater 2008;84:408–14.
[33] Freytes DO, Tullius RS, Valentin JE, Stewart-Akers AM, Badylak SF. Hydrated versus lyophilized forms of porcine extracellular matrix derived from the urinary bladder. J Biomed Mater Res A 2008;87:862–72.
[34] Freytes DO, Tullius RS, Badylak SF. Effect of storage upon material properties of lyophilized porcine extracellular matrix derived from the urinary bladder. J Biomed Mater Res B Appl Biomater 2006;78:327–33.
[35] Keane TJ, Londono R, Turner NJ, Badylak SF. Consequences of ineffective decellularization of biologic scaffolds on the host response. Biomaterials 2012; 33:1771–81.
[36] Brown BN, Valentin JE, Stewart-Akers AM, McCabe GP, Badylak SF. Macrophage phenotype and remodeling outcomes in response to biologic scaffolds with and without a cellular component. Biomaterials 2009;30: 1482–91.
[37] Valentin JE, Stewart-Akers AM, Gilbert TW, Badylak SF. Macrophage participation in the degradation and remodeling of extracellular matrix scaffolds. Tissue Eng Part A 2009;15:1687–94.
[38] Ishii KJ, Akira S. Innate immune recognition of, and regulation by, DNA. Trends Immunol 2006;27:525–32.
[39] Gilbert TW, Freund JM, Badylak SF. Quantification of DNA in biologic scaffold materials. J Surg Res 2009;152:135–9.
[40] Goto N. Discriminative staining methods for the nervous system: luxol fast blue–periodic acid-Schiff–hematoxylin triple stain and subsidiary staining methods. Stain Technol 1987;62:305–15.
[41] Reing JE, Brown BN, Daly KA, Freund JM, Gilbert TW, Hsiong SX, et al. The effects of processing methods upon mechanical and biologic properties of porcine dermal extracellular matrix scaffolds. Biomaterials 2010;31: 8626–33.
[42] Reing JE, Zhang L, Myers-Irvin J, Cordero KE, Freytes DO, Heber-Katz E, et al. Degradation products of extracellular matrix affect cell migration and proliferation. Tissue Eng Part A 2009;15:605–14.
[43] Greene LA, Tischler AS. Establishment of a noradrenergic clonal line of rat adrenal pheochromocytoma cells which respond to nerve growth factor. Proc Natl Acad Sci U S A 1976;73:2424–8.
[44] Rydel RE, Greene LA. Acidic and basic fibroblast growth factors promote stable neurite outgrowth and neuronal differentiation in cultures of PC12 cells. J Neurosci 1987;7:3639–53.
[45] Santos SD, Verveer PJ, Bastiaens PI. Growth factor-induced MAPK network topology shapes Erk response determining PC-12 cell fate. Nat Cell Biol 2007; 9:324–30.
[46] Hall FL, Fernyhough P, Ishii DN, Vulliet PR. Suppression of nerve growth factor-directed neurite outgrowth in PC12 cells by sphingosine, an inhibitor of protein kinase C. J Biol Chem 1988;263:4460–6.
[47] Allan G, Krakowka S, Ellis J, Charreyre C. Discovery and evolving history of two genetically related but phenotypically different viruses, porcine circoviruses 1 and 2. Virus Res. Available from: URL, http://www.ncbi.nlm.nih.gov/pubmed/21945213; 2012.
[48] Mankertz A, Persson F, Mankertz J, Blaess G, Buhk HJ. Mapping and characterization of the origin of DNA replication of porcine circovirus. J Virol 1997; 71:2562–6.
[49] Paul PS, Halbur P, Janke B, Joo H, Nawagitgul P, Singh J, et al. Exogenous porcine viruses. Curr Top Microbiol Immunol 2003;278:125–83.
[50] Zeev-Brann AB, Lazarov-Spiegler O, Brenner T, Schwartz M. Differential effects of central and peripheral nerves on macrophages and microglia. Glia 1998;23: 181–90.
[51] Lazarov-Spiegler O, Solomon AS, Schwartz M. Peripheral nerve-stimulated macrophages simulate a peripheral nerve-like regenerative response in rat transected optic nerve. Glia 1998;24:329–37.
[52] Vijayraghavan S, Wang M, Birnbaum SG, Williams GV, Arnsten AF. Inverted-U dopamine D1 receptor actions on prefrontal neurons engaged in working memory. Nat Neurosci 2007;10:376–84.
[53] Mendes FA, Onofre GR, Silva LC, Cavalcante LA, Garcia-Abreu J. Concentration-dependent actions of glial chondroitin sulfate on the neuritic growth of midbrain neurons. Brain Res Dev Brain Res 2003;142:111–9.
[54] Endeman D, Kamermans M. Cones perform a non-linear transformation on natural stimuli. J Physiol 2010;588:435–46.
[55] Agrawal V, Tottey S, Johnson SA, Freund JM, Siu BF, Badylak SF. Recruitment of progenitor cells by an extracellular matrix cryptic peptide in a mouse model of digit amputation. Tissue Eng Part A 2011;17:2435–43.
[56] Tottey S, Corselli M, Jeffries EM, Londono R, Peault B, Badylak SF. Extracellular matrix degradation products and low-oxygen conditions enhance the regenerative potential of perivascular stem cells. Tissue Eng Part A 2011;17: 37–44.
[57] Freytes DO, Martin J, Velankar SS, Lee AS, Badylak SF. Preparation and rheological characterization of a gel form of the porcine urinary bladder matrix. Biomaterials 2008;29:1630–7.
[58] Hong Y, Huber A, Takanari K, Amoroso NJ, Hashizume R, Badylak SF, et al. Mechanical properties and in vivo behavior of a biodegradable synthetic polymer microfiber-extracellular matrix hydrogel biohybrid scaffold. Biomaterials 2011;32:3387–94.